62nd JANNAF Propulsion Meeting (7th Spacecraft Propulsion), Nashville, TN, 1–5 June, 2015

PROPULSION UNIT FOR CUBESATS (PUC)

D. L. Carroll[1], J. M. Cardin[2], R. L. Burton[1], G. F. Benavides[1], N. Hejmanowski, [1] C. Woodruff[1], K. Bassett[1], D. King[1], J. Laystrom-Woodard[1], L. Richardson[1], C. Day[2], K. Hageman[2], and R. Bhandari[2]

[1]CU Aerospace, Champaign, IL

[2]VACCO Industries, South El Monte, CA

ABSTRACT

The CU Aerospace/VACCO Industries Propulsion Unit for CubeSats (PUC) was developed as a medium thrust, medium impulse thruster system to enable CubeSat orbital maneuvering, formation flying, and rendezvous. The 0.25U PUC casing is all-welded titanium, and comes fully integrated with all necessary propulsion subsystems, including controller, power processing unit, micro-cavity discharge thruster, propellant valves, heaters, sensors, and software. The unit is software-configurable to operate over a wide range of power, thrust, and impulse levels. System setpoints, system status, and firing telemetry are accessible and configurable through an RS422 serial interface. The baseline system fits within a compact 350 cm^3 volume (0.25U+"hockey puck"), with an 89 mm x 89 mm cross-section, leaving clearance for solar panels and magnetic torquers. PUC may be expanded from 0.25U to any desired length, providing significant potential for increased propellant capacity and ΔV capability, compared with the baseline 0.25U design. The 0.25U PUC draws 15 W when using a microcavity discharge (MCD) to heat the high-density, self-pressurizing liquid SO_2 propellant, coupled to an optimized micronozzle to provide 5 mN thrust at 70 s I_{sp}, a 4 kg CubeSat ΔV of 48 m/s, and demonstrates negligible component wear and constant lifetime operations. A dedicated propellant heater provides for continuous operation below +5°C ambient temperature. Cold gas operation can be used for small impulse operations. On-orbit update of system parameters is provided, including thrust duration, plenum pressure, MCD power level temperature & fault set-points.

1. INTRODUCTION

An emerging trend in the field of space exploration is the development and deployment of low mass satellites, commonly referred to as micro-, nano-, or femto-satellites. These satellites are seeing increasing use as a low-cost alternative to more traditional large-scale spacecraft, a notable example being the CubeSat standard, and eventually as components in a durable, redundant satellite network. Nanosats are designed for a life of 1-2 years. They often have body-mounted solar panels, which makes them severely power limited, with usable specific power P/m of ~1 watt per kg of satellite mass (note that the Lockheed-Martin A2100 bus used for geosynchronous satellites has 4000 W capability and a launch mass of ~3000 kg, so the 1 W/kg rule of thumb holds over a wide range of satellite masses). CubeSats are also volume limited (1 liter per cube), placing a severe volume constraint on the propulsion system. Nanosats are a low-cost, easily replaced approach to satellite constellations, and as such need to be nimble. That is, orbital maneuvers need to be accomplished relatively quickly to minimize mission control costs and maximize the usable satellite duty cycle of 1-2 years. Although rapid orbital maneuvering can

Work funded by AFRL/RQRS on contract FA9300-11-C-0007.

 Paper Tracking # 4059

always be accomplished by chemical propulsion, scaling down chemical systems to nanosat size (thrust << 1 Newton) has proved difficult for solid and liquid propulsion systems. Thus, one impediment to wide implementation of nanosats is the lack of a highly compact, simple, and efficient propulsion system for primary (orbital transfer, drag makeup, and maneuvering) and secondary (attitude and trajectory control) applications. Advances at the University of Illinois in using microcavity plasma discharges for illumination [Eden, 2005; Park, 2005] provide a possible solution to this problem in the form of a Microcavity Discharge (MCD) thruster [Burton, 2009; Burton, 2010; Burton, 2012]. Unlike previous attempts at microdischarge propulsion systems that failed because they operated in an arc mode, the MCD thruster operates in a very low electrode erosion normal or abnormal glow discharge mode at high voltage and low current. This new technology can revolutionize low-power electric propulsion for femto-, pico-, nano-, micro- and even larger satellites to perform various mission tasks including orbit transfer, de-orbiting, station-keeping, position, attitude and acceleration control, and structure control.

Our motivation for adapting MCD technology to the micropropulsion field is the expected system benefits of high specific thrust, high thrust density, and high specific power with high propellant utilization and a simple power processor. These aspects of MCD technology are desirable for a number of reasons. First, an MCD thruster operates at the low power levels available on nanosatellites [Ghosh, 2010]. Additionally the MCD thruster is capable of generating higher thrust than other forms of electric propulsion which increases the operational lifetime of a typical nanosatellite. For very small scale electrothermal thrusters gas heating to temperatures in excess of 1000 K is possible with microdischarges. The microdischarge gas temperature can be tuned to range from ambient values to high values by changing the power input. The overall thruster efficiency is predicted to be greater than 60% using monatomic gas propellants, and power scalability is straightforward over a wide range by operating large numbers of abnormal glow discharges in parallel. Additionally, the service lifetime of the thruster is expected to be long due to operation in the glow discharge mode and the capability of operating without auxiliary components.

Other advantages of the MCD thruster include:

1. Power is coupled via the normal or abnormal glow discharge, so electrodes remain relatively cool, and heat loss is minimized.
2. The system incorporates capacitively-coupled and/or direct-coupled electrodes, minimizing sheath loss and electrode ablation.
3. Electrode erosion is very low, because the ion sputtering erosion mechanism is significantly reduced by operating in low current normal or abnormal glow discharge modes.
4. Low wall heat loss due to a wall area on the order of 0.1 – 1.0 mm^2 per cavity.
5. Ionization fraction is <<1% and small resulting frozen flow losses.
6. No auxiliary systems are needed, e.g. neutralizer, heater, igniter.
7. Propellant is stored as a self-pressurizing liquid, and is evaporated to provide an operating pressure is 0.1 – 1.0 atm, giving reasonable nozzle Reynolds numbers, low viscous losses, and mN thrust levels [Bayt, 1999].
8. High stagnation temperatures are possible with the MCD (1500 K has been obtained with Al/Al_2O_3 insulators), much higher than attainable with the resistojet, without the need for bulky, inefficient thruster insulation.
9. The power processing unit (PPU) is comprised of a DC-AC inverter or pulsed DC power supply with low mass (≈ 3 g/W), and with PPU efficiency exceeding 85%.
10. Throttleable by varying source pressure.
11. Very low thrust noise, making it a candidate for missions requiring extremely precise, low-noise acceleration control.
12. Very low system mass and volume for use on low mass (<10 kg) satellites.

This paper reviews prior MCD thruster results, motivations for the technology, and presents performance data taken with the CU Aerospace/VACCO 0.25U Propulsion Unit for CubeSats (PUC), a robust system based upon MCD thruster technology.

2. BACKGROUND AND DISCUSSION

EARLY MCD THRUSTER DESIGN AND EXPERIMENTS

The early version of the MCD thruster [Burton, 2009; Burton, 2010], **Figs. 1 and 2**, is an electrothermal thruster composed of a gaseous propellant supply and feed system, two or more Al/Al_2O_3 electrodes powered by a 50-500 kHz, 400-1600 V AC supply, a 100-200 μm diameter cavity in which the discharge plasma is created, and a moderate Reynolds number micronozzle [Bayt, 1999]. The key technology behind the MCD Thruster is the MEMs-scale plasma discharge. Over the past decade, it has been found that low temperature plasma confined to a microcavity has several remarkable properties, including specific power loadings (i.e., volumetric power deposition into the plasma) of up to ~1000 W/mm^3 on a steady state basis, operating pressures of less than 100 Torr to above one atmosphere, and electron temperatures of 3-6 eV. This region of the parameter space has not previously been accessible to plasma science but it is already clear that these parameters open entirely new applications of plasma technology.

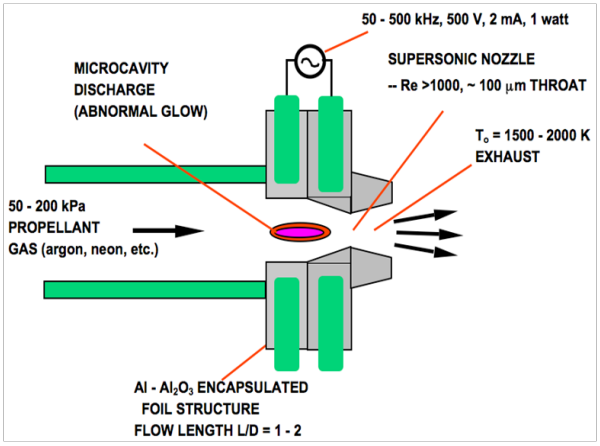

Fig. 1. Schematic of original design of an MCD electrothermal microthruster.

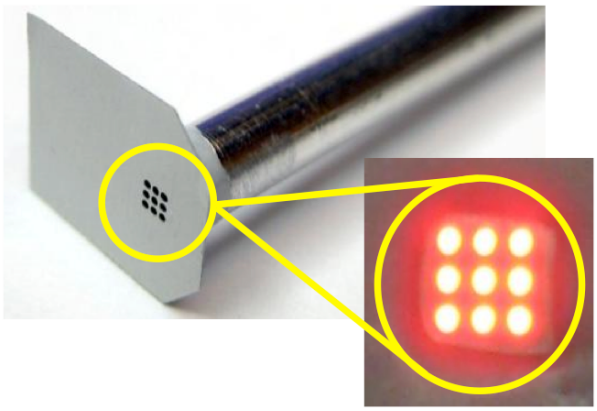

Fig. 2. Photograph of early stage development MCD electrothermal microthruster with foil electrodes. Inset shows unit in operation.

In early versions, the basic structure of the MCD thruster was composed of two or more electrodes stacked in a 'sandwich' configuration with a microcavity drilled or etched through the stack. The electrodes were created by growing an oxide layer on pure aluminum foils. The microcavity can be either drilled using a commercially available micro drill bit, or created with a wet chemical etching process, for cavities having characteristic dimensions as small as 10 μm. The foils were then aligned and connected together using an epoxy resin, and then connected to a chemically etched nozzle. This effort was supported by numerical modeling of the microdischarges [Sitaraman, 2010] to better understand the dominant physical mechanisms.

Previously published work on the MCD thruster using gaseous propellants, typically argon, neon, nitrogen, or a mixture thereof focused on power levels in the 1 – 5 W range [Burton, 2009; Burton, 2010; de Chadenedes, 2010]. These studies included thrust estimates and thermal efficiency measurements. The highest efficiency reached to date is 50%, with 60% predicted [de Chadenedes, 2010]. Lifetime issues were prevalent in the early stage development MCD thrusters with the foil structure; the thin insulation would typically develop microcracks during operation that would ultimately result in shorting and arcing in the flowing system. As such, CU Aerospace used Internal Research and Development funds to explore a modification of the MCD thruster that consisted of replacing the insulator with a more robust oxide tube. With the implementation of the dielectric tube several configurations are possible for the

electrodes for initiating and sustaining an alternating current normal or abnormal glow discharge [Burton, 2012].

NANOSATELLITE THRUSTER CHOICES

An important question for nanosatellites is: what range of efficiency and specific impulse are appropriate for a nanosat electric micropropulsion system? TRL 9 EP systems have flown with efficiency η (%) and specific impulse I_{sp} (s) including the pulsed plasma thruster (10%, 1000 s); the resistojet (50-80%, 300 s); the Hall thruster (50%, 2000 s); and the ion thruster (70%, 3000 s). Other EP systems in advanced development are the colloid thruster; and the FEEP thruster. Propulsion selection for nanosats depends on the propulsion capability, expressed in terms of the maneuver time and the required orbital maneuver expressed in terms of ΔV, and also on the mass and volume available for the propulsion system on the nanosat.

Burton *et al.* [Burton, 2010] introduced an equation for a constrained maneuver time that showed ΔV varying *inversely* with U_e; a priori, this is counterintuitive because high ΔV interplanetary missions typically utilize high specific impulse systems. The conclusion is that, in order to minimize orbit transfer times, *more maneuver capability is available for propulsion systems with low exhaust velocity and specific impulse.* To insist incorrectly on a high specific impulse is to incur a long time to perform the maneuver or to limit the ΔV capability of the nanosat.

Clearly, the maneuver time t is a fundamentally important parameter. The question then is what maneuver time is appropriate? Because we are dealing with low-cost nanosats with limited design life (1-2 years) in a rapid response environment, it is not useful to have maneuver times of weeks or months and their associated delayed response, high mission control support costs and satellite downtimes. It is more reasonable that the time to perform a maneuver should be measured in days. **Figure 3** illustrates some typical values of ΔV per day for a maneuverable nanosat, as a function of I_{sp}. We assume that $\eta\phi \sim 0.50$ (where ϕ is the power fraction P_p/P, defined in terms of the propulsive power P_p, and the maximum nanosat bus power P produced by the solar panels), P/m ~ 1 W/kg, and that the desired time for a single maneuver is 1.0 days.

As discussed by Burton *et al.* [Burton, 2010], the "sweet spot" for nanosat orbital maneuvers (shaded region) appears to be in the 70 – 400 s range of I_{sp}, where ΔV is relatively large but the fuel fraction is reasonably small, **Fig. 3**. For 50 s, typical of cold gas thrusters, ΔV is high but fuel fraction is too large. For 2000 s, assuming a 50% efficient Hall thruster, the ΔV per day is only 4.3 m/s; for 3000 s, assuming a 50% efficient ion thruster, the ΔV per day is only 2.9 m/s; and for a 6000 s FEEP thruster, the ΔV per day is only 1.5 m/s. These latter ΔV values are too small to be useful in time-constrained maneuvers. The colloid thruster could eventually be considered assuming significant improvements in efficiency and system volume.

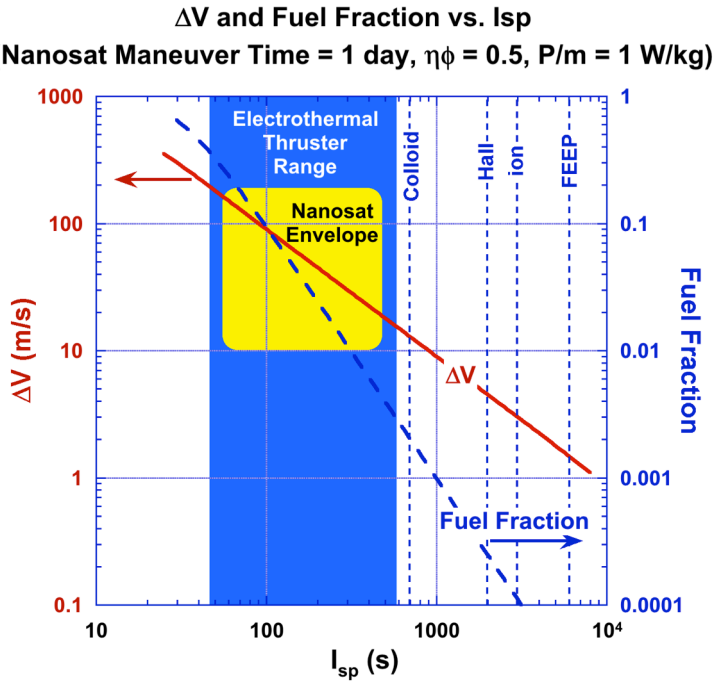

Fig. 3. Operating envelope for nanosat propulsion. Maneuver time is one day, requiring high thrust and reducing specific impulse to the electrothermal range.

We note that a nanosat propulsion system can operate from batteries. For a 5 kg, 5 W nanosat operating for one day, the required energy is 432 kJ = 120 W-hr. Lithium-ion batteries of this size would

have a mass of about 1 kg, or 20% of the satellite mass, making battery operation possible, but requiring a large fraction of the total nanosat mass. Batteries could be used in conjunction with photovoltaic cells to increase power and decrease maneuver time, effectively providing $\phi > 1$.

Unlike low power ion and Hall thrusters, which incur a large efficiency penalty from their neutralizers, electrothermal thrusters in principle can operate at high efficiency at low I_{sp}. The reason that ion and Hall thrusters need high I_{sp} to be efficient is that the exhaust is fully ionized, so that the kinetic energy of the exhaust must be large compared to the energy required (ion cost) to ionize the xenon propellant. Low power electrothermal thrusters on the other hand have no inherent requirement for highly ionized propellant, which can be made sufficiently conductive with an ionization fraction of 10^{-3} – 10^{-6}.

The conclusion from this discussion is that the best specific impulse range for nanosats is relatively low, in a range favoring electrothermal thrusters, **Fig. 3**.

PROPELLANT SELECTION

Propulsion performance is critically dependent on the propellant choice. A number of propellants have been considered for CubeSats, including isobutane (C_4H_{10}), nitrous oxide (N_2O), propane, ammonia, hydrazine, peroxide, refrigerants (R134a), etc. [London, 2010]. CU Aerospace executed a study of 350 candidate propellants for the CubeSat/nanosatellite propulsion application, and down-selected to 8 candidates. Selection is based on the following criteria, **Tables 1 and 2**. Another common refrigerant R236fa is also a potential candidate; while it has several differences to R134a (most notably molecular weight and lower vapor pressure), it is overall similar to R134a in estimated total performance numbers and is not discussed further in this paper. (Note that SO_2 has also previously been denoted as EP-13.)

Table 1: Criteria for best candidate nanosatellite propellants.

Criterion	Justification	Favorable for	Not favorable for
High liquid density ρ	max propellant mass and ΔV	Water, SO_2, R134a	NH_3, N_2O, C_4H_{10}
High ρ x sound speed	max ΔV	H_2O, N_2H_4, SO_2, NH_3, R134a	SF_6, N_2O, C_4H_{10}
Low heat of vaporization	low propellant heater power	SO_2, R134a	H_2O, N_2H_4, NH_3
Self-pressurizing	simplifies feed system	SO_2, NH_3, R134a	H_2O, N_2H_4, N_2O
Critical temperature >60°C	liquid between 0°C and 60°C	H_2O, SO_2, NH_3, R134a	N_2H_4, SF_6, N_2O, C_4H_{10}
Low freezing point	liquid between 0°C and 60°C	SO_2, NH_3, R134a	H_2O, N_2H_4
Compatible with materials & electronics	Enables location of electronics inside storage tank	R134a, C_4H_{10}, SO_2	H_2O, NH_3
Overall Selection	**Optimizes Propulsion System**	**SO_2, R134a**	**H_2O, N_2H_4, NH_3, SF_6, N_2O, C_4H_{10}**

Because both cold and warm gas could be used, the primary selection criterion is the product ρa of liquid density times sound speed at 300 K, or equivalently the product of liquid density and maximum cold I_{sp}, **Table 2**. A secondary criterion is the propellant heat of vaporization.

The third criterion is self-pressurization capability, which eliminates the need for a separate pressurization system, saves mass and volume, and therefore increases propellant mass and impulse. Propellants are selected with sufficient vapor pressure at 0ºC and modest pressure at 60ºC to avoid excessive tank wall thickness and mass (note that thicker tank walls can significantly reduce propellant volume in the small tank sizes necessitated for nanosatellites). Propellants with a critical temperature below 60ºC (SF_6, N_2O, C_4H_{10}) are avoided because the initial tank fill must be low to avoid over-pressurization at 60ºC.

Table 2: Comparison of product of liquid density and 90% of maximum I_{sp} at 500°C for nanosatellite propellants.

Propellant	Mol. Weight (g/mole)	Density (g/cm^3)	Isp at 500°C & 90% Nozzle Eff. (s)	Density x Isp ($g\text{-}s/cm^3$)	Issues
H_2O	18	1.002	155.1	155.4	Freezes @ 0°C, low vapor pressure
N_2H_4	32	1.008	116.3	117.2	Toxic, Freezes @ 2°C
SO_2	64	1.381	82.2	113.6	Manageable Low toxicity
NH_3	17	0.609	159.5	95.2	High P @ 60°C, thick structure
R134a	102	1.225	65.1	79.8	None
N_2O	44	0.785	99.2	77.8	Critical temperature < 60°C
SF_6	146	1.374	54.4	74.8	Critical temperature < 60°C
C_4H_{10}	58	0.579	86.4	50.0	Low liquid density, $T_{critical}$ < 60°C

The fourth criterion is materials compatibility with the feed system, thruster and with the control and power electronics. While not strictly required, this capability gives the most volume-efficient way to package electronics, inside the propellant tank, while providing waste heat to maintain propellant pressure and temperature while evaporating. Testing studies performed by CU Aerospace have identified materials that are compatible with R134a and SO_2.

Finally, freezing is a concern for a tank temperature of 0ºC for H_2O and N_2H_4, requiring that this risk be mitigated by thermal management and propellant heating. These two propellants, despite high ρa, are also contraindicated by high heat of vaporization and low self-pressurization. Because nanosatellites/CubeSats are generally power limited, the additional heater power required during lengthy LEO eclipse times could significantly impact these nanosatellites. Of the investigated propellants, the two most appealing for the CubeSat operating temperature range of 0 – 60 °C are R134a and SO_2. Note that SO_2 was a common refrigerant until the mid-1920's when CFC-based refrigerants were introduced. With the exception of its low toxicity, SO_2 has excellent refrigerant characteristics and it is these characteristics that also make it an excellent propellant that is compatible with the MCD thruster technology.

3. EXPERIMENTAL RESULTS WITH PUC PROTOTYPE

EXPERIMENTAL SETUP

Experiments were performed with a conical thruster nozzle having a 0.015" (0.38 mm) throat just downstream of the microcavity discharge region. The basic configuration tested is illustrated in **Fig. 4**, for which the plenum, MCD, PPU, and nozzle were all in a compact test housing, **Fig. 5**. Thrust stand measurements were performed by placing the compact test housing on a Watt linkage pendulum thrust platform with non-intrusive wires and gas feed line. The thrust stand has a large amount of prior historical usage [Wilson, 1997; Laystrom, 2003]. Windage effects [Whalen, 1987] were observed from gas recirculation in the medium sized vacuum tank when background pressures were < 10^{-5} Torr, so thrust stand measurements were taken with a background pressure of approximately 160 milli-Torr. As such, measurements of thrust include a small correction (typically < 5%) for the background pressure.

$$F_{vacuum} = F_{measured} + P_{measured} A_{exit}$$

A photograph of the thruster in operation is shown in **Fig. 6**.

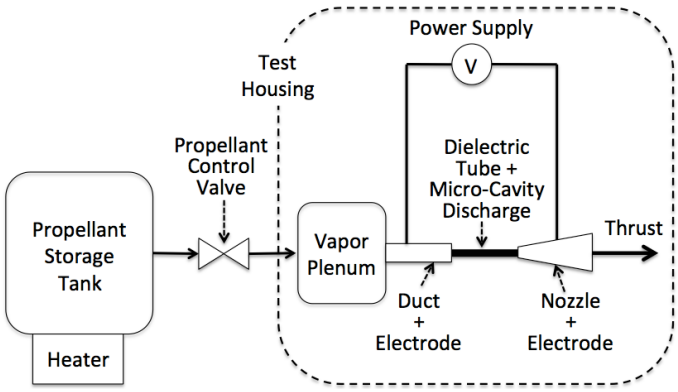

Fig. 4. Schematic of basic robust prototype PUC thruster system. The components within the dashed region were tested inside the test housing.

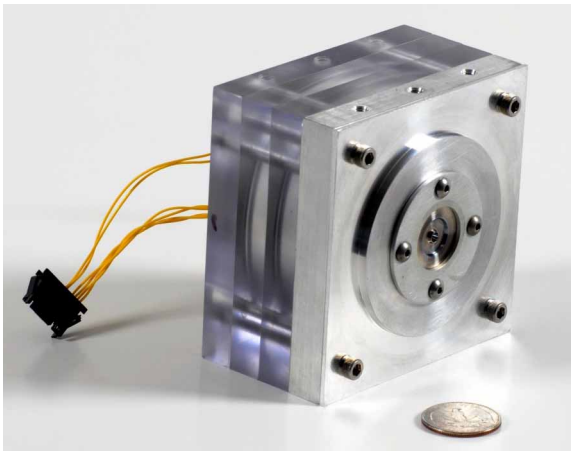

Fig. 5. Photograph of prototype PUC thruster in test housing.

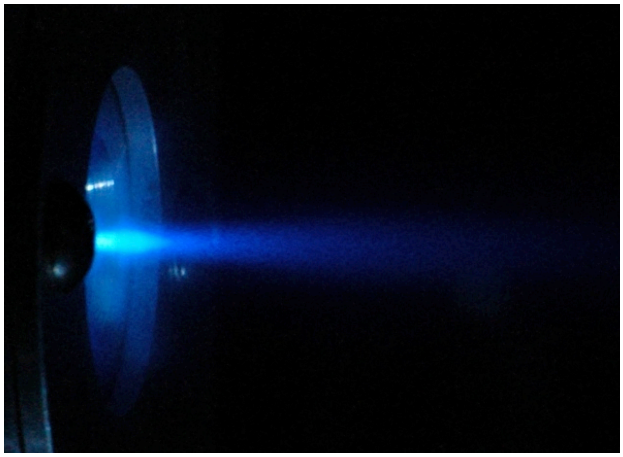

Fig. 6. Photograph of prototype PUC thruster in operation using SO_2.

EXPERIMENTAL DATA

In the laboratory the MCD thruster operates at constant mass flow rate and allows the static pressure to increase as the total temperature increases. Knowing mass flow rate and the discharge coefficient C_D allows the total temperature of the discharge to be inferred from comparison between the pressure and mass flow measurements:

$$T_0^* = \frac{\gamma}{R}\left(\frac{\gamma+1}{2}\right)\left(\frac{p^* A_{eff}}{\dot{m}}\right)^2$$

where R is the gas constant, γ depends upon the total temperature, $A_{eff}^* = C_D A^*$, $p_0^* \cong p_0$, and the throat pressure is given by:

$$p^* = p_0\left(2/(\gamma+1)\right)^{\frac{\gamma}{\gamma-1}}$$

Experimentally, a cold gas measurement was made followed by ignition of the MCD and a warm gas measurement taken for the same mass flow rate. Since the mass flow rate and discharge coefficient are experimentally fixed, an increase in line pressure (assumed to be the stagnation pressure since the incoming flow Mach number is < 0.1) corresponds to a rise in discharge stagnation temperature by the

above equations and can therefore be determined without the need for direct measurements other than the pressure. Thus, neglecting a small correction due to variations in γ, $T_0 \sim p^2$, or

$$\left(\frac{T^*_{0,warm}}{T^*_{0,cold}}\right) = \left(\frac{p^*_{0,warm}}{p^*_{0,cold}}\right)^2$$

Measurement of the cold and warm pressures along with the assumption that the cold stagnation temperature is room temperature provides an estimated total temperature in the discharge region downstream of the discharge.

Cold and Warm Gas Performance Data

Plenum pressures using SO_2 propellant are shown in **Fig. 7**, as well as estimated total temperatures in the discharge region (using the above equation) just upstream of the throat, **Fig. 8**. Note that **Fig. 8** shows that the total temperature decreases with mass flow for approximately a constant input power of 10 W, as the same amount of power is being deposited into a progressively larger amount of gas flow.

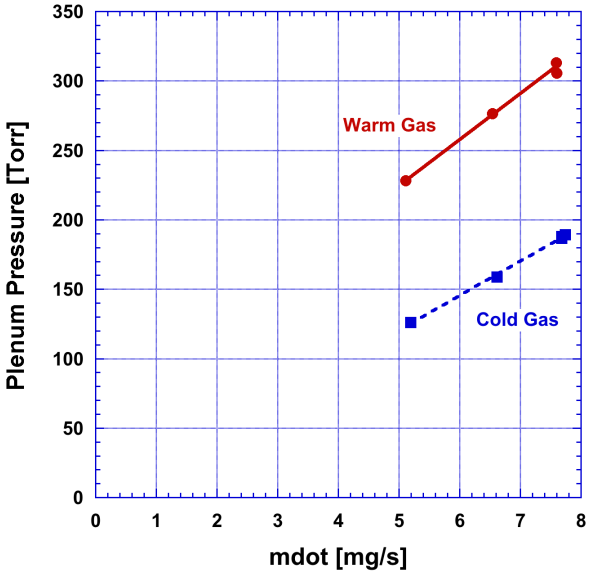

Fig. 7. Plenum pressure of prototype PUC thruster operating in cold gas and warm gas modes.

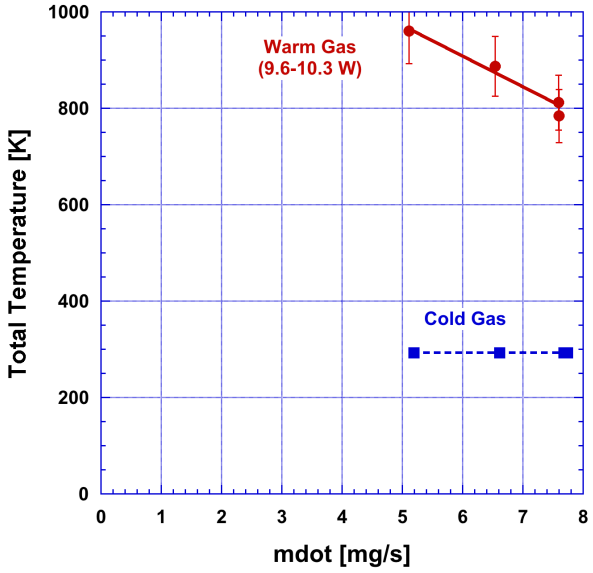

Fig. 8. Estimated total temperature in discharge region of prototype PUC thruster operating in cold gas and warm gas modes (for approximately a constant input power of 10 W).

Thrust stand measurements including the small correction for the windage effects are shown in **Figs. 9 and 10**. The nominal operating flow rate of 7.6 mg/s of propellant indicates a thrust of 3.5 mN and an I_{sp} of 46 s in cold gas mode, and a thrust of approximately 5.4 mN and an I_{sp} of 72 s in warm gas MCD discharge mode. This represents a significant 54% rise in thrust and specific impulse with the highly compact MCD configuration. Cold gas performance was also tested at a much higher flow rate of 14.6 mg/s (not shown for brevity) and produced a thrust of 7.6 mN and an I_{sp} of 52 s. Cold flow thrust stand measurements were also performed with R134a (molecular weight = 102), and display a similar trend to that of SO_2 (molecular weight = 64), but with the anticipated reduced specific impulse (**Section 4**). Note that R134a was found to be incompatible with the MCD warm fire operation due to dissociation of the R134a molecules and subsequent plugging of the nozzle.

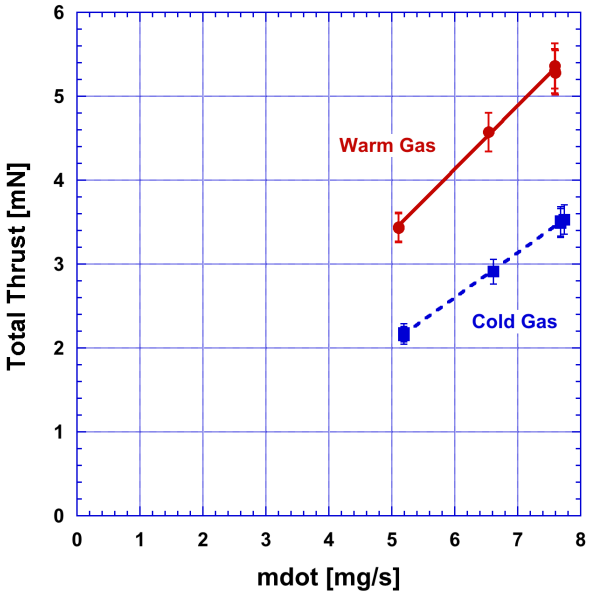

Fig. 9. Measured thrust of prototype PUC thruster operating in cold gas and warm gas modes.

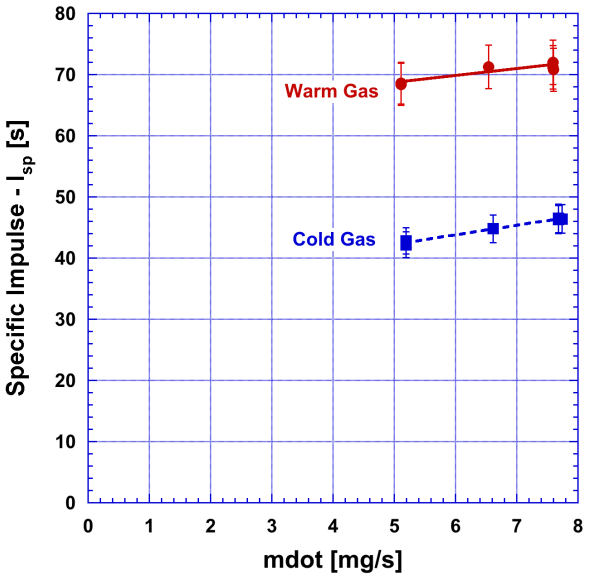

Fig. 10. Measured specific impulse of prototype PUC thruster operating in cold gas and warm gas modes.

Dissociation of the molecular propellant almost certainly plays some role in discharge inefficiencies. The bond energy to dissociate the first O atom from the molecule is 5.676 eV [Takacs, 1978], which corresponds to a power loss of 8.6 W for every 1 mg/s that has the first bond broken. Experiments have not been performed to determine quantitatively the amount of bond dissociation occurring in these MCD tests, but we estimate that it is < 5%, i.e. greater than 95% of the flow is undissociated.

Testing of the MCD was also performed for several different input powers to the PPU. **Figure 11** illustrates the general rise in total temperature of the discharge flow as a function of the ratio of power input to the PPU to the mass flow rate. A more limited set of thrust stand measurements was made for higher specific powers that seemed the most promising, **Fig. 12**. To within experimental error, the specific impulse was approximately a constant for specific powers in the range of 1.2 – 1.8 W/mg/s.

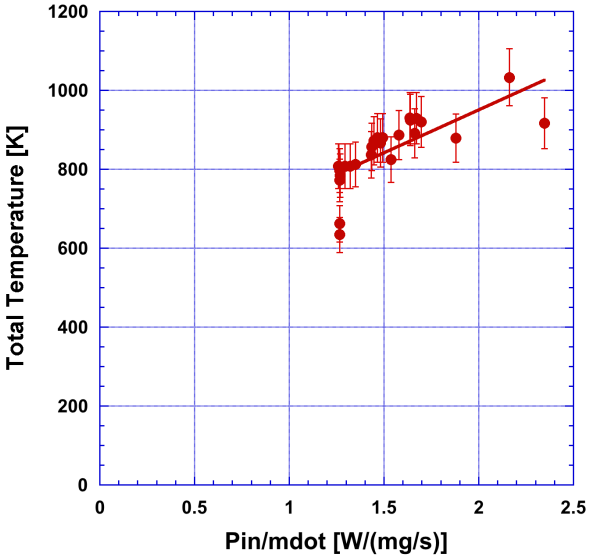

Fig. 11. Estimated total temperature in discharge region of prototype PUC thruster operating in warm gas mode as a function of the specific energy in the discharge region.

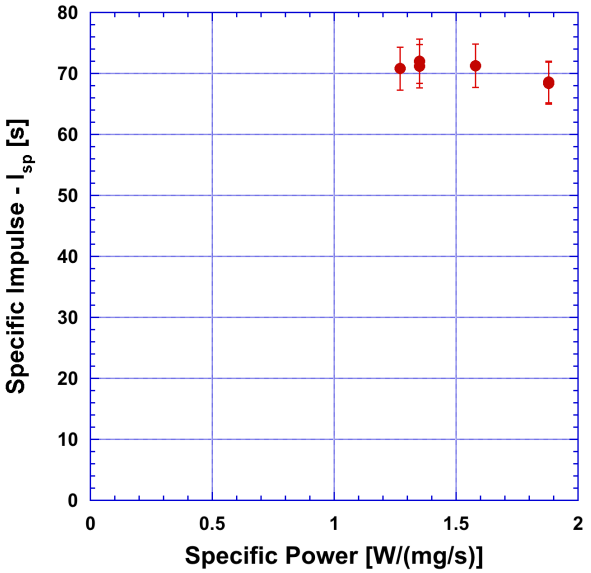

Fig. 12. Measured specific impulse of prototype PUC thruster operating in warm gas mode as a function of the specific energy in the discharge region.

To test the durability of the thruster system a 19-hour continuous test was performed, **Figs. 13-16**, which exceeds the available tank propellant in the PUC system described in **Section 4**. The flow rate for this test was held approximately constant at 7.9 mg/s. An earlier model of our PPU with slightly lower efficiency was utilized in this 19-hour experiment, so performance is slightly decreased from that shown in **Figs. 7-10**, but the differences are < 5%. Interestingly, the thrust performance increased with operational time, possibly due to gradual heating of the entire test housing in which the gas flows into the discharge region. Microscope investigation of the thruster after the 19-hour test showed no plugging or erosion of the nozzle.

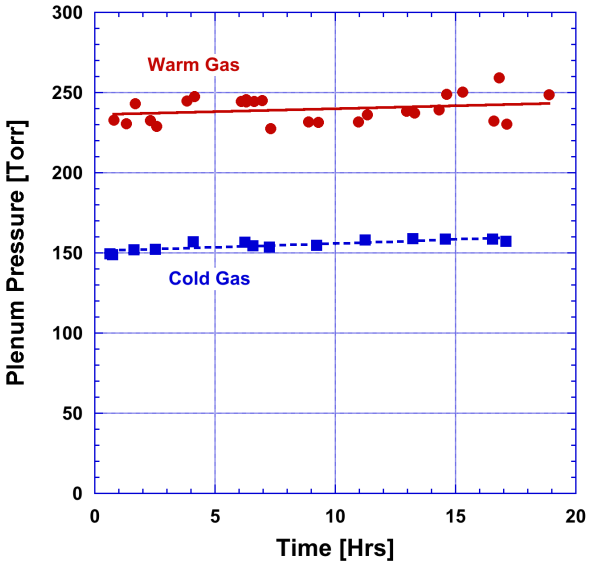

Fig. 13. Plenum pressure of prototype PUC thruster operating in cold gas and warm gas modes during a 19-hour test.

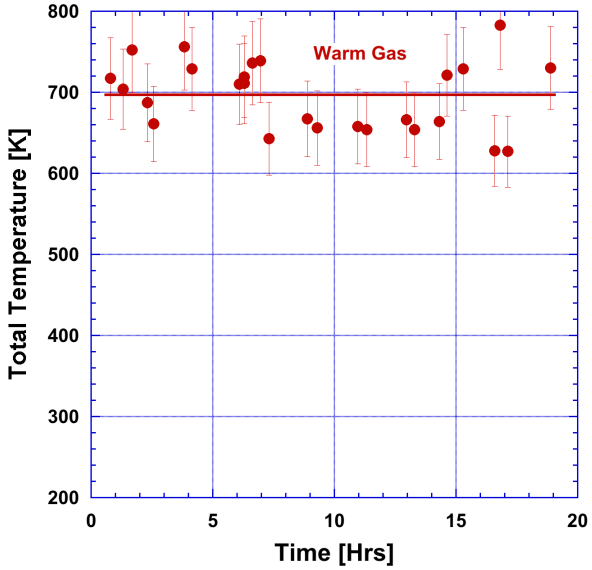

Fig. 14. Estimated total temperature in discharge region of prototype PUC thruster operating in warm gas mode during a 19-hour test.

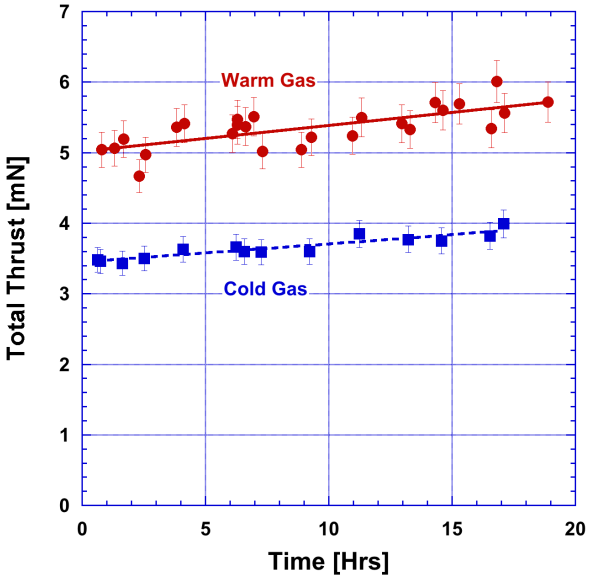

Fig. 15. Measured thrust of prototype PUC thruster operating in cold gas and warm gas modes during a 19-hour test.

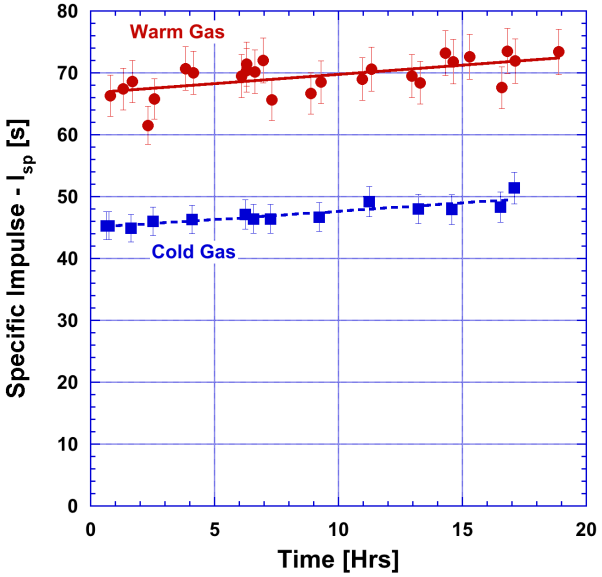

Fig. 16. Measured specific impulse of prototype PUC thruster operating in cold gas and warm gas modes during a 19-hour test.

Discharge coefficients typically ranged from 0.84 – 0.90 for this nozzle, depending upon flow conditions. Nozzle efficiencies typically ranged from 0.80 – 0.90, again depending upon flow conditions.

4. PUC FLIGHT SYSTEM

DESCRIPTION OF PUC FLIGHT SYSTEM

The CU Aerospace / VACCO Propulsion Unit for CubeSats (PUC) is a complete high-performance and compact small-satellite propulsion solution, Fig. 17. The all-welded titanium PUC comes fully integrated with all necessary propulsion subsystems, including controller, power processing unit, micro-cavity discharge thruster, propellant valves, heaters, sensors, and software. PUC is software-configurable to operate over a wide range of power, thrust, and impulse levels. System set-points, system status, and firing telemetry are all accessible and configurable through an RS422 serial interface.

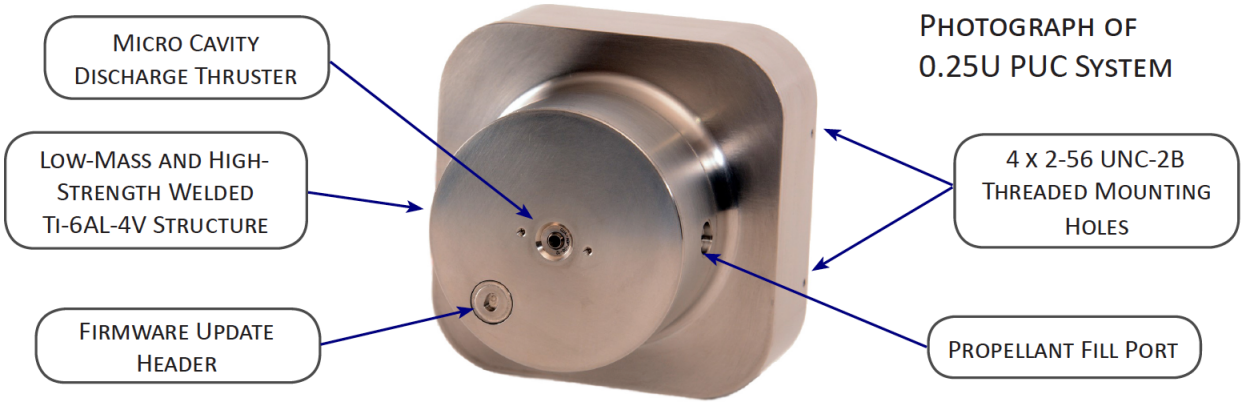

Fig. 17. Photograph of 0.25U PUC flight system showing locations of MCD thruster, propellant fill port, firmware update header and mounting holes in a welded titanium structure. The propellant tank is included in the structure.

The baseline 0.25U system fits within a compact 350 cm^3 volume (0.25U + "hockey puck"), providing outstanding performance for minimal CubeSat volume and mass fraction. The PUC's 89 mm x 89 mm cross-section intentionally falls well under the CubeSat 100 mm x 100 mm specification, so as to not interfere with other CubeSat subsystems such as solar panels and magnetic torquers. For increased performance, or to meet customer specific mission requirements, the tank width may be customized. The tank may additionally be expanded from 0.25U to any desired length, providing significant potential for increased propellant capacity, i.e. delta-V capability, compared with the baseline 0.25U design.

The PUC achieves its high total impulse, low-volume capability by employing CU Aerospace Micro-Cavity Discharge (MCD) propellant heating technology, high-density and self-pressurizing liquid propellants, and an optimized low-mass-flow nozzle. PUC MCD thrusters demonstrate negligible component wear during 0.25U life cycle testing, providing constant lifetime operations. The robust MCD components permit extensive warm firing beyond the 0.25U operational life, allowing for pre-flight testing and/or increases to the PUC's propellant tankage without impacting MCD performance or reliability. PUC system performance estimates are given in **Tables 3 and 4**. The system envelope and dimensions are provided in **Fig. 18** along with center of gravity estimates. Other PUC system specification (mechanical, propellant, and electrical) are provided in the **Appendix**.

Table 3. Performance specifications of 0.25U PUC MCD thruster system in cold (14.6 mg/s flow rate) and warm (7.6 mg/s flow rate) gas modes.

Parameter	Warm Fire Only	Cold Fire Only	Unit	Notes
Thrust	4.5	5.5	mN	Nominal
Total impulse	184	124	N-s	
Delta-V capability (4 kg CubeSat)	48	32	m/s	
Delta-V capability (3 kg CubeSat)	64	43	m/s	
Specific impulse	70	47	sec	Nominal
Maximum continuous thrust time	20	54	min	
Minimum impulse bit	---	1.0	mN-s	

Table 4. Performance of 0.25U PUC MCD thruster system in cold (14.6 mg/s flow rate) and warm (7.6 mg/s flow rate) gas modes as a function of CubeSat launch mass.

CubeSat Launch Mass (kg)	ΔV in Cold Gas Mode (m/s)	ΔV in Warm Gas Mode (m/s)
1.5	86	127
2.0	64	95
3.0	43	64
4.0	32	48
5.0	26	39

System Features

Operation:

- Two operational modes:
- Warm gas mode for high specific impulse, large total impulse manuevers.
- Cold gas mode for minimum or small total impulse manuvers.
- Highly configurable controller for on-orbit update of system parameters, including:
- Thrust duration
- Plenum pressure (thrust)
- MCD power level (specific impulse)
- Temperature set-points
- Fault set-points
- System status packets for health monitoring
- Regular telemetry packets during operation
- Dedicated propellant heater for continous operation below +5°C ambient temperature.
- Propellant temperature sensor for closed-loop propellant temperature regulation.
- Propellant vaporizer ensuring 100% vapor delivered from liquid storage.

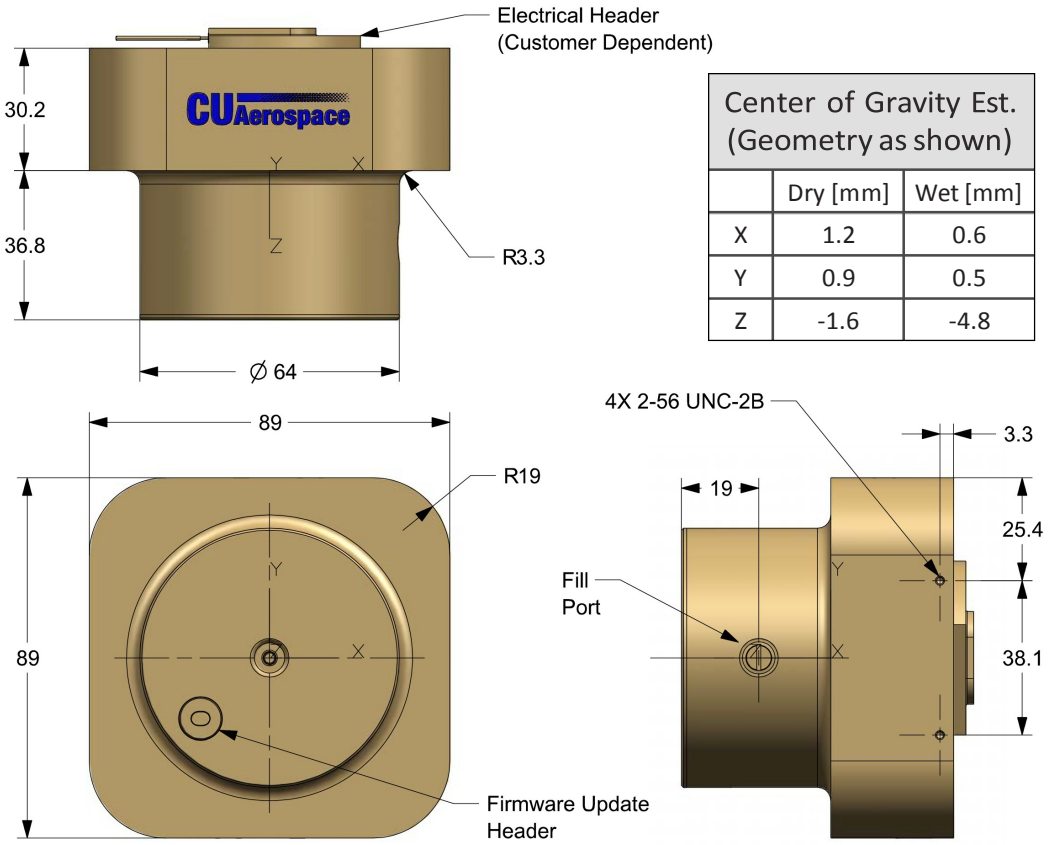

Center of Gravity Est. (Geometry as shown)		
	Dry [mm]	Wet [mm]
X	1.2	0.6
Y	0.9	0.5
Z	-1.6	-4.8

Fig. 18. Envelope and dimensions of the 0.25U PUC flight system including center of gravity estimates.

Sulfur dioxide (SO_2) characteristics:

- High mass density
- Self-pressurizing
- Non-flammable
- Chemically stable
- High critical temperature
- Low freezing point
- Low vapor pressure
- Commonly used refrigerant prior to the development of freons

The hardware is readily adaptable to a variety of propellant tank sizes to provide a family of possible PUC systems, **Fig. 19**. **Table 5** provides estimates of performance with the larger tank sizes for a 4 kg CubeSat.

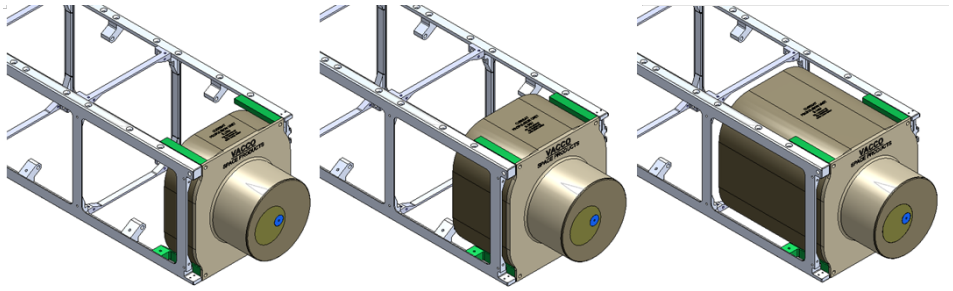

Fig. 19. Family of MCD PUC thruster systems with different propellant tank sizes (0.25U, 0.5U, and 1U sizes are illustrated).

Table 5. Estimated performance of PUC MCD thruster systems for a 4 kg CubeSat launch mass in cold (14.6 mg/s flow rate) and warm (7.6 mg/s flow rate) gas modes as a function of PUC tank size.

PUC Size (Units)	ΔV in Cold Gas Mode (m/s)	ΔV in Warm Gas Mode (m/s)
0.25	32	48
0.5	51	74
0.75	74	109
1.0	97	144

PUC FLIGHT SYSTEM EXPERIMENTAL DATA

Eight PUC flight systems were fabricated, tested and delivered to the Air Force in 2014. Acceptance testing of each of these systems was performed. Plenum pressures using SO_2 and R134a propellants are shown in **Fig. 20**. Thrust stand measurements with both of these propellants (including the small correction for the windage effects) are shown in **Figs. 21 and 22**. As noted earlier, R134a was found to be incompatible with the MCD warm fire operation due to dissociation of the R134a molecules and subsequent plugging of the nozzle, and was therefore only tested in cold gas mode. Operation of all units was within desired specifications.

We note that it should be possible to push the performance to higher thrust and I_{sp} in the warm gas MCD discharge mode with continued optimization of the geometry and electronics. Our estimates are that a total temperature of 1200 K is achievable for which we expect an I_{sp} > 75 s.

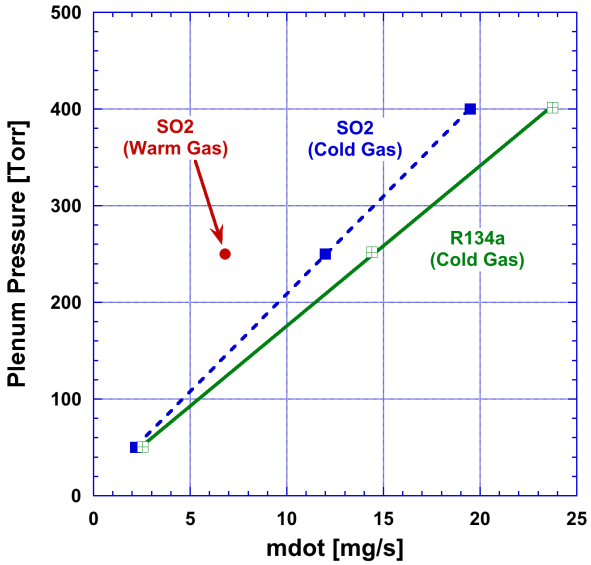

Fig. 20. Plenum pressure of flight PUC thruster operating in cold gas and warm gas modes with SO2 and in cold gas mode with R134a.

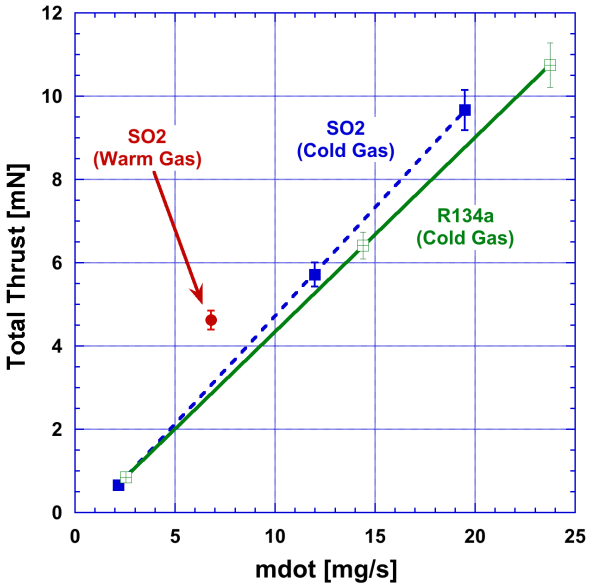

Fig. 21. Measured thrust of flight PUC thruster operating in cold gas and warm gas modes with SO2 and in cold gas mode with R134a.

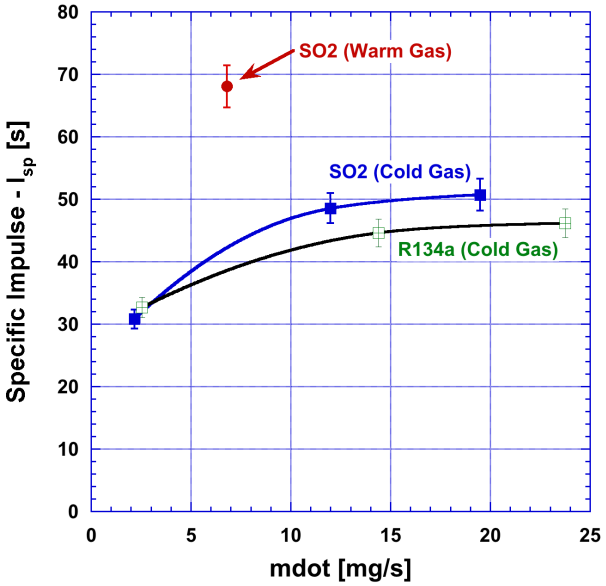

Fig. 22. Measured specific impulse of flight PUC thruster operating in cold gas and warm gas modes with SO2 and in cold gas mode with R134a.

5. CONCLUDING REMARKS

As nanosatellites become an increasingly utilized tool in space missions, the need for a compact and efficient propulsion system becomes ever greater. The Propulsion Unit for CubeSats (PUC) thruster system represents a bridge for the unique needs of the nanosatellite propulsion gap: MCD devices are extremely compact, smaller than virtually any other propulsion system. MCD thrusters are capable of operation in power-limited systems, and MCD thrusters are capable of providing the total impulse levels necessary for nanosatellite missions when utilizing self-pressurizing liquid propellants.

Sulfur dioxide was chosen as an ideal propellant for CubeSats because of its excellent set of characteristics that compensate for CubeSat limitations. Thrust stand measurements using SO_2 propellant showed a thrust of approximately 4.5 mN and an I_{sp} of 46 s in cold gas mode, and a thrust of approximately 5.4 mN and an I_{sp} of 70 s in warm gas MCD discharge mode. This represents a significant >50% rise in performance with the highly compact MCD configuration as compared with cold gas operation. The robust MCD thruster system was tested in a 19-hour experiment and demonstrated no degradation in performance, and no erosion of the electrodes, insulator or nozzle. The PUC system using MCD thruster technology, was fabricated, tested and delivered to the Air Force by the CU Aerospace and VACCO Industries team and represents the first compact (< 0.75U), high total impulse nanosatellite propulsion system. The PUC can be built as a family of thruster systems having a variety of propellant tank sizes to meet the needs of different nanosatellite missions.

6. ACKNOWLEDGEMENTS

This work has been sponsored by the United States Air Force Research Laboratory/RQRS contract number FA9300-11-C-0007. James Singleton and William Hargus served as Program Managers during different phases of the project, and we would also like to acknowledge their timely and important technical contributions.

7. REFERENCES

Bayt, R. L., **Analysis, Fabrication and Testing of a MEMS-based Micropropulsion System**, PhD thesis, Department of Aeronautics and Astronautics, MIT. (1999)

Burton, R. L., Eden, J. G., Park, S.-J., Yoon, J. K., de Chadenedes, M., Garrett, S., Raja, L. L., Sitaraman, H., Laystrom-Woodard, J., Benavides, G., and Carroll, D., Proceedings of the 31st International Electric Propulsion Conference, **Initial Development of the Microcavity Discharge Thruster**, IEPC-2009-169. (2009)

Burton, R. L., Eden, J. G., Park, S.-J., de Chadenedes, M., Garrett, S., Raja, L. L., Sitaraman, H., Laystrom-Woodard, J., Benavides, G., and Carroll, D., "**Development of the MCD Thruster for Nanosat Propulsion**," JANNAF Conf., Colorado Springs, CO, Paper 1387 (2010).

Burton, R. L., Benavides, G.F., and Carroll, D.L., "**Space Thruster Using Robust Microcavity Discharge**," U.S. Patent Application No. 13/680,484 (2012).

de Chadenedes, M., Yoon, J.K., Sitaraman, H., Garrett, S., Raja, L.L., Eden, J.G., Park, S-J, Laystrom-Woodard, J., Carroll, D.L., and Burton, R.L., **"Advances in Microcavity Discharge Thruster Technology,"** AIAA Paper 2010-6616 (2010).

Eden, J. G., Park, S. –J., Ostrom, N. P., Chen, K. -F., Kim, K. S. "**Large Arrays of Microcavity Plasma Devices for Active Displays and Backlighting,**" *IEE/OSA Journal of Display Technology*, Vol. 1, No. 1, pp. 112-116. (2005)

Ghosh, A, Coverstone, V. "**Study of Low-Thrust Trajectories for Low Orbit Multiple CubeSat Missions**," AAS conference, paper no. 10-174 (2010).

Laystrom, J.K., Burton, R.L., and Benavides, G.F., **"Geometric Optimization of a Coaxial Pulsed Plasma Thruster,"** AIAA Paper 2003-5025 (2003).

London, A. P., and Droppers, L. J., "High-Performance Liquid Propulsion For CubeSats: Requirements and Approaches," JANNAF Conf., Colorado Springs, CO, Paper 1428 (2010).

Park, S.-J., Kim, K. S., Eden, J. G. "**Nanoporous Alumina as a Dielectric for Microcavity Plasma Devices: Multilayer Al/Al_20_3 Structures**," *Applied Physics Letters*, Vol. 86, No. 22, pp. 1-3. (2005)

Sitaraman, H. and Raja, L., **Simulation Studies of Alternating-Current Microdischarges for Microthruster Applications,** AIAA Paper No. AIAA-2010-231. (2010)

Takacs, G.A., **"Heats of Formation and Bond Dissociation Energies of Some Simple Sulfer- and Halogen-Containing Molecules,"** J. Chem Eng. Data, Vol. 23, No. 2, 174-175 (1978).

Whalen, M.V., "**Low Reynolds Number Nozzle Flow Study**," NASA-TM-100130 (1987).

Wilson, M.J., Bushman, S.S., and Burton, R.L., **"A Compact Thrust Stand for Pulsed Plasma Thrusters,"** 25th International Electric Propulsion Conf., IEPC Paper 97-122, Cleveland, OH (1997).

APPENDIX: PUC SPECIFICATIONS

Mechanical Specifications (0.25U System)

Parameter	Minimum	Nominal	Maximum	Unit	Notes
Dimensions	89 mm x 89 mm x 67 mm (0.25U + “hockey puck”)				
Wet mass		718		g	nominal
Dry mass		450		g	nominal
Temperature ranges					
Operating	-13		+50	°C	
Storage w/o propellant	+5		+50	°C	recommended preflight storage
Storage w/ propellant	+5		+30	°C	recommended preflight storage
Survivability	-34		+71	°C	flight
Pressure ranges (propellant tank)					
Operating pressure	20	48	122	psia	
Proof pressure	317			psia	
Burst pressure	528			psia	
Vibe acceptance level	14			G_{RMS}	
Leak rates					
Isolation valve (NC)		5	19	g/yr	1 g/yr = 0.04 scch
Proportional valve (NC)		5	19	g/yr	1 g/yr = 0.04 scch
Mass flow regulation (throttle capability)					
Cold fire	20	100	200	%	of nominal
Warm fire	80	100	120	%	of nominal

Propellant Specifications

Parameter	Value	Unit	Notes
Propellant	SO_2		High Purity Liquid Sulfur Dioxide
Propellant mass (0.25U System)	268	g	Nominal
Critical temperature	156.9	°C	
Freezing point	-75.6	°C	
Vapor pressure	48	psia	At 20°C

Electrical Specifications

Parameter	Minimum	Nominal	Maximum	Unit	Notes
Operating voltage	9	11.1	12.6	V	Unregulated
Max transient voltage			14	V	
Max in-rush current			14.5	A	> 7 amps for less than 50 ms
DC isolation resistance	0.99	1	1.01	MΩ	
Power					
Warm Fire	12	15	18	W	User programmable
Cold Fire	5.9	8	9.8	W	Input voltage dependent
Standby		0.01	0.05	W	
Communication standard	RS422 (115.2 kbps)				
Electrical Wiring (Flying Leads)					
26 AWG PTFE (24” min.)	Blue	Green	Orange	Yellow	Red (x2)	Black (x2)
Purpose	RS422_Y	RS422_Z	RS422_A	RS422_B	9-12.6 V	GND
Firmware Update Header					
Pin #	1	2	3	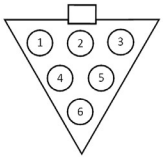	
Purpose	3.3V	TDO	TDI		
Pin #	4	5	6		
Purpose	TMS	TCK	GND		